NUCL SCI TECH (2016) 27:21
DOI 10.1007/s41365-016-0023-8

Asymmetric neutron stars in the presence of vacuum fluctuations

Hong-Hui Guan[1] · Chen Wu[2] · Ji-Feng Yang[1,3]

Received: 13 January 2016 / Revised: 1 February 2016 / Accepted: 5 February 2016 / Published online: 2 March 2016

Abstract The asymmetric neutron stars are investigated in a relativistic effective model with vacuum fluctuations (VF) taken into account. Due to the VF effects, various properties of the neutron matter become 'softened' comparing to that obtained in the FSUGold model, and the maximum mass of the $(npe\mu)$ neutron stars is reduced from $1.71M_{\odot}$ to $1.35M_{\odot}$.

Keywords Neutron star · Relativistic mean-field theory · Vacuum fluctuation · Equation of state

1 Introduction

The neutron stars with masses of the order of solar mass are the result of supernova explosions. As their radii are merely 10–12 km [1], the interior density of a neutron star exceeds several times the nuclear saturation density. Thus, neutron star matter provides an interesting laboratory for studying strong interactions at high density of nucleons and has been attracting a lot of academic interests [2–4]. In this work, we will concentrate our investigation on the asymmetric neutron stars consisting of neutrons, protons, and leptons.

The basic framework to be employed is the relativistic mean-field theory (RMF) that has proven successful for the study of nuclear matter as a relativistic many-body system of baryons and mesons [5, 6]. Ever since the seminal work of the Walecka model [5], there have been many important extensions of quantum hadron dynamics (QHD) that improved our understanding of hadron matter at high density. For example, an important theoretical advancement appeared in early 2001 [7], where nonlinear couplings between the isovector and isoscalar mesons were introduced to soften the symmetry energy of nuclear matter at high density using an appropriate data set called the FSUGold model [8]. Further applications of this model and its extensions proved to be successful in many aspects [9–11].

As noted in Ref. [12], it is better to use the in-medium meson masses in such RMF studies of nuclear matter at high density (Actually such in-medium meson masses have been studied in both experimental and theoretical approaches [13–18]). Following Refs. [12, 19], we will calculate the effective masses of nucleons. Mesons are calculated by taking into account the effects of the vacuum fluctuation (VF) in the extension of QHD proposed in Refs. [7, 8]. We will also investigate how the properties of neutron matter are affected. Our results will be compared to these obtained in the FSUGold model [20, 21].

This work is organized as follows: In Sect. 2, we present the framework (henceforth referred to as VF-RMF model as in Ref. [19]) and theoretical results for our investigation of various properties for neutron stars. In Sect. 3, the numerical results are presented in comparison with that of FSUGold model. The summary is given in Sect. 4.

✉ Ji-Feng Yang
jfyang@phy.ecnu.edu.cn

1 Department of Physics, East China Normal University, Shanghai 200241, China

2 Shanghai Institute of Applied Physics, Chinese Academy of Sciences, Shanghai 201800, China

3 Kavli Institute for Theoretical Physics China, Chinese Academy of Sciences, Beijing 100190, China

2 Effective masses and nuclear matter

The Lagrangian density employed in this work reads [21]

$$\begin{aligned}\mathcal{L} = &\sum_N \bar{\psi}_N\Big(i\gamma^\mu\partial_\mu - m_N + g_{\sigma N}\sigma - g_{\omega N}\gamma^\mu\omega_\mu - \frac{g_{\rho N}}{2}\gamma^\mu\vec{\tau}\cdot\vec{\rho}_\mu\Big)\psi_N \\ &+\frac{1}{2}\partial^\mu\sigma\partial_\mu\sigma - \frac{1}{2}m_\sigma^2\sigma^2 - \frac{\kappa}{3!}(g_{\sigma N}\sigma)^3 \\ &-\frac{\lambda}{4!}(g_{\sigma N}\sigma)^4 - \frac{1}{4}F^{\mu\nu}F_{\mu\nu} + \frac{1}{2}m_\omega^2\omega^\mu\omega_\mu + \frac{\zeta}{4!}\left(g_{\omega N}^2\omega^\mu\omega_\mu\right)^2 \\ &+\frac{1}{2}m_\rho^2\vec{\rho}^\mu\cdot\vec{\rho}_\mu - \frac{1}{4}\vec{G}^{\mu\nu}\cdot\vec{G}_{\mu\nu} \\ &+\Lambda_v\left(g_{\rho N}^2\vec{\rho}^\mu\cdot\vec{\rho}_\mu\right)\left(g_{\omega N}^2\omega^\mu\omega_\mu\right) + \sum_l \bar{\psi}_l(i\gamma^\mu\partial_\mu - m_l)\psi_l,\end{aligned} \tag{1}$$

where N represents nucleons n and p, and l represents leptons e^- and μ^-, m_N, m_σ, m_ω, and m_ρ denote the masses for N and σ, ω, ρ, respectively. $F_{\mu\nu}$ and $\vec{G}_{\mu\nu}$ denote the antisymmetric tensors of vector fields ω and ρ, respectively [21]. Note that Λ_v is the coupling first introduced in Ref. [7].

The meson field equations in the RMF read:

$$m_\sigma^2\sigma + \frac{1}{2}\kappa g_{\sigma N}^3\sigma^2 + \frac{1}{6}\lambda g_{\sigma N}^4\sigma^3 = \sum_N g_{\sigma N}\rho_N^S, \tag{2}$$

$$m_\omega^2\omega + \frac{\zeta}{6}g_{\omega N}^4\omega^3 + 2\Lambda_v g_{\rho N}^2 g_{\omega N}^2\rho^2\omega = \sum_N g_{\omega N}\rho_N, \tag{3}$$

$$m_\rho^2\rho + 2\Lambda_v g_{\rho N}^2 g_{\omega N}^2\omega^2\rho = \frac{1}{2}\sum_N g_{\rho N}\tau_{3N}\rho_N, \tag{4}$$

where ρ_N and ρ_N^S are the nucleon density and scalar density, respectively,

$$\rho_N = 2\int_0^{k_F^N}\frac{d^3k}{(2\pi)^3}, \tag{5}$$

$$\rho_N^S = -i\int\frac{d^4k}{(2\pi)^4}\mathrm{Tr}[G_D^N(k)], \tag{6}$$

with k_F^N being the Fermi momentum of the nucleon and G_D^N being the in-medium part of the propagator for quasi-nucleons,

$$G^N(k) \equiv G_F^N(k) + G_D^N(k), \tag{7}$$

$$G_F^N(k) \equiv \frac{\gamma^\mu k_\mu + m_N^*}{k^2 - (m_N^*)^2 + i\epsilon}, \tag{8}$$

$$G_D^N(k) \equiv i\pi\frac{\gamma^\mu k_\mu + m_N^*}{E_F^N}\delta(k^0 - E_F^N)\theta(k_F^N - |\vec{k}|), \tag{9}$$

where $E_F^N \equiv \sqrt{(k_F^N)^2 + (m_N^*)^2}$ and m_N^* is the effective mass that includes the VF effects as below (Fig. 1a)[12, 19]:

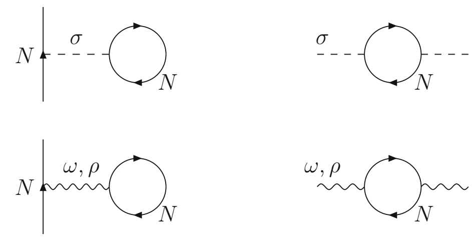

Fig. 1 The one-loop self-energy of nucleons (**a**) and mesons (**b**)

$$\begin{aligned}m_N^* = &m_N + \frac{g_{\sigma N}^2}{(m_\sigma^*)^2}\left\{i\int\frac{d^4k}{(2\pi)^4}\mathrm{Tr}[G^n(k) + G^p(k)]\right. \\ &\left.+\frac{\kappa(m_N^* - m_N)^2}{2} - \frac{\lambda(m_N^* - m_N)^3}{6}\right\} \\ =\ &m_N + \frac{g_{\sigma N}^2 m_N^*}{2\pi^2(m_\sigma^*)^2}\left\{(m_N^*)^2\ln\frac{(k_F^n + E_F^n)(k_F^p + E_F^p)}{m_N^2}\right. \\ &-k_F^nE_F^n - k_F^pE_F^p. + \frac{m_N^3}{m_N^*}\left[2 - \frac{2m_N^*}{m_N}\right. \\ &\left.\left.-\left(5 - \frac{\pi^2\kappa}{m_N}\right)\left(1 - \frac{m_N^*}{m_N}\right)^2 + \frac{11 + \pi^2\lambda}{3}\left(1 - \frac{m_N^*}{m_N}\right)^3\right]\right\}.\end{aligned} \tag{10}$$

The effective (in-medium) meson masses are calculated in the random-phase approximation (RPA) (Fig. 1b) [22],

$$(m_\sigma^*)^2 = m_\sigma^2 + \Pi_\sigma(q), \tag{11}$$

$$(m_i^*)^2 = m_i^2 + \Pi_{i,T}(q), (i = \omega, \rho), \tag{12}$$

with $\Pi_{i,T}$ being the corresponding transverse part of the polarization tensor of vector mesons,

$$\Pi_\sigma(q) = -ig_{\sigma N}^2\sum_N\int\frac{d^4k}{(2\pi)^4}\mathrm{Tr}\left[G^N(k+q)G^N(k)\right], \tag{13}$$

$$\Pi_{\omega,\mu\nu}(q) = -ig_{\omega N}^2\sum_N\int\frac{d^4k}{(2\pi)^4}\mathrm{Tr}\left[\gamma_\mu G^N(k+q)\gamma_\nu G^N(k)\right], \tag{14}$$

$$\Pi_{\rho,\mu\nu}(q) = -i\frac{g_{\rho N}^2}{4}\sum_N\int\frac{d^4k}{(2\pi)^4}\mathrm{Tr}\left[\tau_N\gamma_\mu G^N(k+q)\tau_N\gamma_\nu G^N(k)\right], \tag{15}$$

with which one could obtain on-shell and off-shell in-medium meson masses. The expressions of the off-shell ($q^\mu = 0$) case are quite simple:

$$\begin{aligned}\Pi_\sigma(q^\mu = 0) = &\frac{3g_{\sigma N}^2}{2\pi^2}\sum_N\left[\frac{(m_N^*)^2k_F^N + \frac{1}{3}(k_F^N)^3}{E_F^N} - (m_N^*)^2\right. \\ &\left.\times\ln\frac{k_F^N + E_F^N}{m_N} + \frac{m_N^2 + 3(m_N^*)^2}{2} - 2m_N^*m_N\right],\end{aligned} \tag{16}$$

$$\Pi_{\omega,T}(q^\mu=0)=\frac{g_{\omega N}^2}{3\pi^2}\sum_N\frac{(k_F^N)^3}{E_F^N},\quad \Pi_{\rho,T}(q^\mu=0)=\frac{g_{\rho N}^2}{24\pi^2}\sum_N\frac{(k_F^N)^3}{E_F^N}. \tag{17}$$

For the asymmetric neutron star matter with nucleons and charged leptons, the β equilibrium conditions are guaranteed with the following relations of chemical potentials:

$$\mu_p=\mu_n-\mu_e,\quad \mu_\mu=\mu_e, \tag{18}$$

and the charge-neutrality condition,

$$n_p=n_e+n_{\mu^-}, \tag{19}$$

where n_i is the number density of particle i, and the chemical potentials of nucleons and leptons read

$$\begin{aligned}\mu_N&=E_F^N+g_{\omega N}\omega+g_{\rho N}\tau_{3N}\rho,\\ \mu_l&=\sqrt{(k_F^l)^2+m_l^2},\end{aligned} \tag{20}$$

where k_F^l denotes the Fermi momentum of a lepton.

Then, the equations of state (EOS) obtained in this VF-RMF model read,

$$\begin{aligned}\varepsilon=&\sum_N\frac{\gamma_N}{(2\pi)^3}\int_0^{k_F^N}\sqrt{(m_N^*)^2+k^2}\mathrm{d}^3k+\frac{1}{2}(m_\omega^*)^2\omega^2\\&+\frac{\zeta}{8}g_{\omega N}^4\omega^4+\frac{1}{2}(m_\sigma^*)^2\sigma^2+\frac{\kappa}{6}g_{\sigma N}^3\sigma^3\\&+\frac{\lambda}{24}g_{\sigma N}^4\sigma^4+\frac{1}{2}(m_\rho^*)^2\rho^2+3\Lambda_v g_{\rho N}^2g_{\omega N}^2\omega^2\rho^2\\&+\frac{1}{\pi^2}\sum_l\int_0^{k_F^l}\sqrt{k^2+m_l^2}k^2\mathrm{d}k\\&-\frac{1}{8\pi^2}\sum_N\Bigg[(m_N^*)^4\ln\frac{m_N^*}{m_N}+m_N^3(m_N-m_N^*)-\frac{7}{2}m_N^2(m_N-m_N^*)^2\\&+\frac{13}{3}m_N(m_N-m_N^*)^3-\frac{25}{12}(m_N-m_N^*)^4\Bigg],\end{aligned} \tag{21}$$

$$\begin{aligned}p=&\sum_N\frac{1}{3}\frac{\gamma_N}{(2\pi)^3}\int_0^{k_F^N}\frac{k^2\mathrm{d}^3k}{\sqrt{(m_N^*)^2+k^2}}+\frac{1}{2}(m_\omega^*)^2\omega^2\\&+\frac{\zeta}{24}g_{\omega N}^4\omega^4-\frac{1}{2}(m_\sigma^*)^2\sigma^2-\frac{\kappa}{6}g_{\sigma N}^3\sigma^3\\&-\frac{\lambda}{24}g_{\sigma N}^4\sigma^4+\frac{1}{2}(m_\rho^*)^2\rho^2+\Lambda_v g_{\rho N}^2g_{\omega N}^2\omega^2\rho^2\\&+\frac{1}{3\pi^2}\sum_l\int_0^{k_F^l}\frac{k^4\mathrm{d}k}{\sqrt{k^2+m_l^2}}\\&+\frac{1}{8\pi^2}\sum_N\Bigg[(m_N^*)^4\ln\frac{m_N^*}{m_N}+m_N^3(m_N-m_N^*)-\frac{7}{2}m_N^2(m_N-m_N^*)^2\\&+\frac{13}{3}m_N(m_N-m_N^*)^3-\frac{25}{12}(m_N-m_N^*)^4\Bigg].\end{aligned} \tag{22}$$

With these EOS, the mass-radius relation, other properties of neutron stars can be computed by solving the Tolman–Oppenheimer-Volkoff (TOV) Eq. [1].

3 Numerical results and discussions

The nucleon and meson masses and the isoscalar couplings of the FSUGold data set, listed in Table 1, are adopted in our calculation. The couplings $(g_{\sigma N}, g_{\omega N}, g_{\rho N})$ are determined so that the following saturation properties are reproduced: nucleon density $\rho_0=0.148\,\mathrm{fm}^{-3}$, binding energy per nucleon $E/A=-16.3\,\mathrm{MeV}$, and the symmetry energy $E_{\mathrm{sym}}=32.5\,\mathrm{MeV}$, they are listed in Table 2 together with the FSUGold data set for comparison.

The effective nucleon mass calculated from Eq. (10) is shown by the solid line in Fig. 2. The decreasing of nucleon effective mass versus nucleon density is slower with the VF effects than that without, in agreement with the findings using other VF-RMF models [12, 19].

Table 1 The parameter set in FSUGold

Parameters	Values
m_σ (MeV)	491.5
m_ω (MeV)	783
m_ρ (MeV)	763
κ	1.42
λ	0.0238
ζ	0.06
Λ_v	0.03

Table 2 Nucleon-meson coupling constants

Coupling	VF-RMF	FSUGold
$g_{\sigma N}$	14.57	10.59
$g_{\omega N}$	12.917	14.3
$g_{\rho N}$	10.29	11.7673

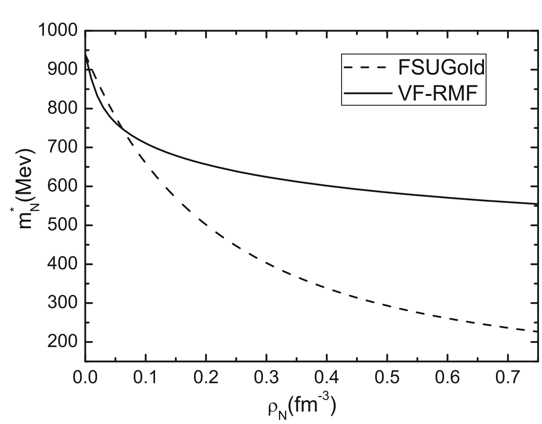

Fig. 2 Effective nucleon mass as a function of nucleon density

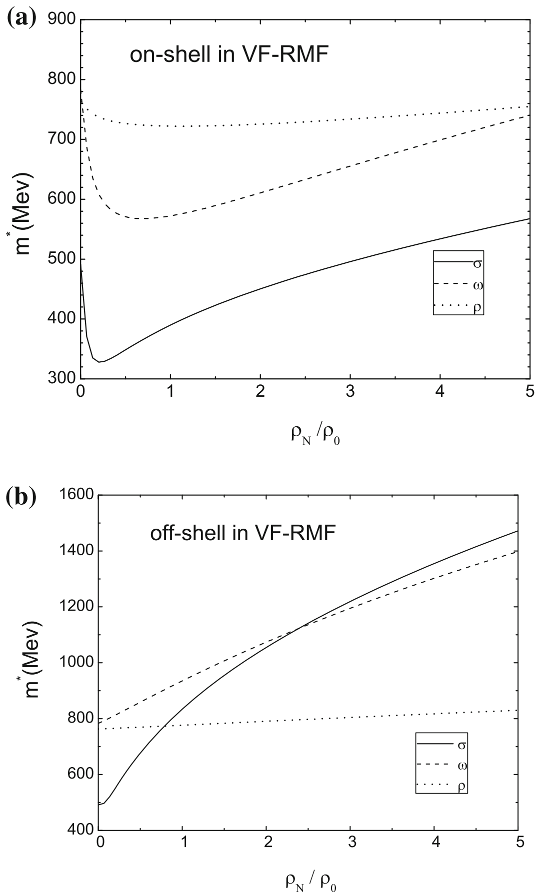

Fig. 3 Effective meson masses: on-shell (**a**) and off-shell (**b**)

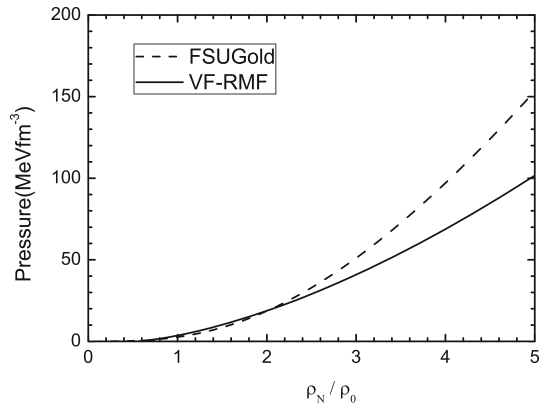

Fig. 4 Equation of state for $(npe\mu)$ matter in VF-RMF and FSUGold models

The effective meson masses (on-shell and off-shell) calculated from Eqs. (11–17) are depicted in Fig. 3. Our results here agree with that of Ref. [19] as the same loop diagrams are involved. We note that the on-shell effective meson masses (Fig. 3a) decrease at the normal density, which are indicated in most experiments and theoretical studies [12–19]. As noted in Ref. [19], the effective meson masses begin to increase at high density, which are beyond the reach of current experiments. As the four-momentum transfer equals zero, the off-shell effective meson masses (Fig. 3b) increase with the nucleon density, which is different from the on-shell ones.

The EOS curve determined from Eqs. (21), (22) (when the neutron star matter reaches β equilibrium) is presented in Fig. 4 together with the curve from the FSUGold model for a comparison. We see again that the EOS curve in our VF-RMF model is lower than that in the FSUGold model, similar to the findings in Ref. [19]. That is to say, the VF effects 'softened' the EOS curve of the asymmetric neutron matter. In Figs. 5 and 6, we presented the particle population for $(npe\mu)$ matter at different nucleon densities in the FSUGold model and VF-RMF model, respectively. The left panel is for $\Lambda_v = 0.03$ and the right panel for $\Lambda_v = 0$. We see that the population curves in Figs. 5 and 6 bear almost the same shapes; the differences are negligible.

Now following standard procedures for solving the TOV equation with the help of EOS, we could obtain the mass (in units of solar mass, $M_\odot$) of the neutron star. The outcome is shown in Fig. 7 and Table 3. The maximum mass of the $(npe\mu)$ neutron stars in our VF-RMF model is $1.35M_\odot$, about 21% down in size compared to the FSUGold value, $1.71M_\odot$ [20], similar to that found in Ref. [19]. The curves obtained in other non-VF models [20] and the two recent astronomical observations, the binary-pulsar systems $J0348+0432$ and $J1614-2230$ [23, 24], were also shown in Fig. 7 for comparison. The implications will be briefly discussed in next section. We note in passing that a quark star with maximum mass over two solar mass was obtained in an improved quasiparticle model in Ref. [25].

4 Conclusion

In summary, we considered the VF effects (from nucleon loop) in the framework of RMF that include additional isoscalar–isovector cross interaction terms for softening the symmetric energy of nuclear matter at high density. For illustration, we considered in this work the simple case of determining the three nucleon-meson couplings $(g_{\sigma N}, g_{\omega N}, g_{\rho N})$ via some saturation properties, while keeping the rest of the parameters of the FSUGold model intact. Like studies using other RMF models, the VF effects tend to 'soften' the EOS curve and other properties of the asymmetric neutron matter, and the maximum mass of such neutron stars is reduced from $1.71M_\odot$ to $1.35M_\odot$.

Given that the recent experimental/observational data of maximum neutron mass is about $2.0M_\odot$ [23, 24], it seems in principle to be a demanding job to explore how other and

Fig. 5 Relative populations in ($npe\mu$) neutron star in FSUGold model

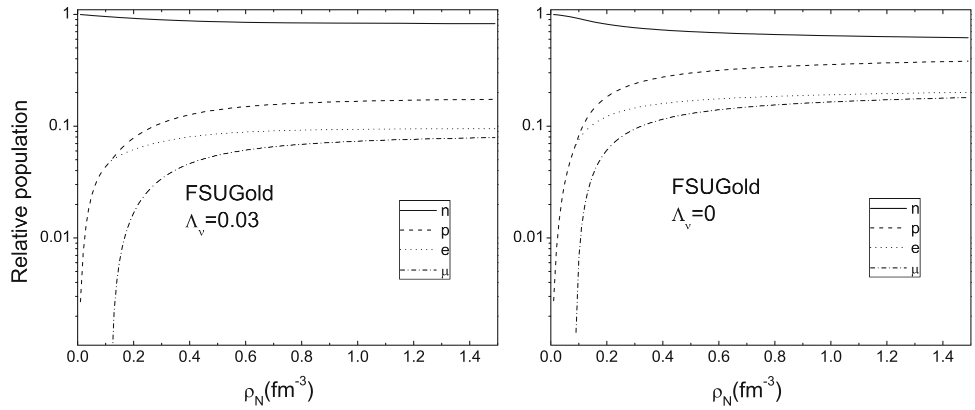

Fig. 6 Relative populations in ($npe\mu$) neutron star in VF-RMF model

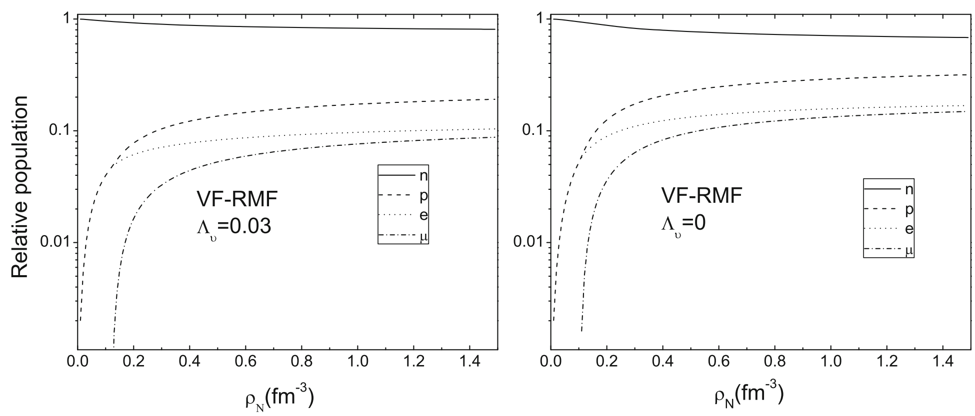

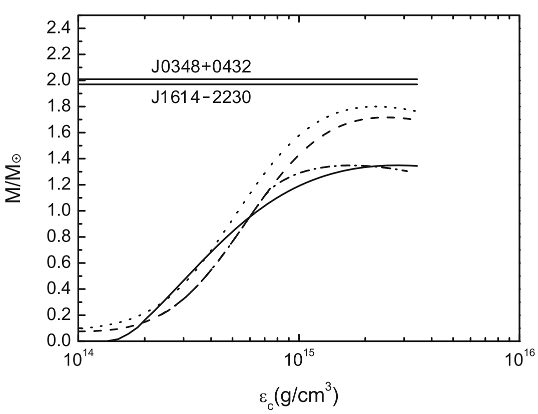

Fig. 7 Neutron star mass versus central density: pure neutron star (*dotted curve*); $npe\mu$ neutron star in FSUGold model (*dashed curve*); $n + p + hyperons$ (*dash-dotted curve*); $npe\mu$ neutron star in VF-RMF (this work) (*solid curve*)

Table 3 The maximum mass in VE-RMF and FSUGold models

Parameter	VF-RMF	FSUGold
$\Lambda_v = 0.03$	$1.35M_{\odot}$	$1.71M_{\odot}$

higher loop corrections within the RMF framework could affect the neutron properties before arriving at reliable theoretical conclusions. As we only determined the coupling constants in a very limited region of the whole parameter space, the results obtained here could not be used to infer too much. Further exploration of other regions of the parameter space for the couplings in Eq. (1) will be done in the near future.

Acknowledgments The study was supported by National Natural Science Foundation of China (No. 11435005) and the Major State Basic Research Development Program in China (No. 2014CB845402).

References

1. N.K. Glendenning, *Compact Stars* (Springer, Berlin, 2000)
2. Z. Zhang, H. Shen, Relativistic equation of state for non-uniform nuclear matter. Nucl. Tech. **37**, 100514 (2014). doi:10.11889/j.0253-3219.2014.hjs.37.100514. **(in Chinese)**
3. M. Yu, K.J. Duan, S.S. Wang et al., A nuclear density probe: isobaric yield ratio difference. Nucl. Sci. Tech. **26**, S20503 (2015). doi:10.13538/j.1001-8042/nst.26.S20503
4. X.Q. Liu, M.R. Huang, R. Wada et al., Symmetry energy extraction from primary fragments in intermediate heavy-ion

collisions. Nucl. Sci. Tech. **26**, S20508 (2015). doi:10.13538/j.1001-8042/nst.26.S20508

5. J.D. Walecka, A theory of highly condensed matter. Ann. Phys. **83**, 491–529 (1974). doi:10.1016/0003-4916(74)90208-5
6. B.D. Serot, J.D. Walecka, in *The Relativistic Nuclear Many-Body Problem*, ed. J. W. Negele, E. Vogt, Adv. Nucl. Phys. Plenum Press **16**, 1 (1986)
7. C.J. Horowitz, J. Piekarewicz, Neutron star structure and the neutron radius of ^{208}Pb. Phys. Rev. Lett. **86**, 5647–5650 (2001). doi:10.1103/PhysRevLett.86.5647
8. B.G. Todd-Rutel, J. Piekarewicz, Neutron-rich nuclei and neutron stars: a new accurately calibrated interaction for the study of neutron-rich matter. Phys. Rev. Lett. **95**, 122501 (2005). doi:10.1103/PhysRevLett.95.122501
9. J. Piekarewicz, Pygmy dipole resonance as a constraint on the neutron skin of heavy nuclei. Phys. Rev. C **73**, 044325 (2006). doi:10.1103/PhysRevC.73.044325
10. J. Piekarewicz, Validating relativistic models of nuclear structure against theoretical, experimental, and observational constraints. Phys. Rev. C **76**, 064310 (2007). doi:10.1103/PhysRevC.76.064310
11. F.G. Fattoyev, J. Piekarewicz, Relativistic models of the neutron-star matter equation of state. Phys. Rev. C **82**, 025805 (2010). doi:10.1103/PhysRevC.82.025805
12. A. Bhattacharyya, S.K. Ghosh, S.C. Phatak, Effect of in-medium meson masses on nuclear matter properties. Phys. Rev. C **60**, 044903 (1999). doi:10.1103/PhysRevC.60.044903
13. G.E. Brown, M. Rho, Scaling effective Lagrangians in a dense medium. Phys. Rev. Lett. **66**, 2720–2723 (1991). doi:10.1103/PhysRevLett.66.2720
14. H. Hatsuda, S.H. Lee, Phys. Rev. C **46**, R34(R) (1992). doi:10.1103/PhysRevC.46.R34
15. S. Sarkar, J. Alam, P. Roy et al., Photons from hadronic matter at finite temperature. Nucl. Phys. A **634**, 206–230 (1998). doi:10.1016/S0375-9474(98)00159-6
16. K. Ozawa, H. En'yo, H. Funahashi et al., Observation of ρ/ω meson modification in nuclear matter. Phys. Rev. Lett. **86**, 5019–5022 (2001). doi:10.1103/PhysRevLett.86.5019
17. D. Trnka, G. Anton, J.C.S. Bacelar et al., Observation of in-medium modifications of the ω meson. Phys. Rev. Lett. **94**, 192303 (2005). doi:10.1103/PhysRevLett.94.192303
18. B. Krusche, In-medium properties of hadrons. Int. J. Mod. Phys. A **22**, 406–415 (2007). doi:10.1142/S0217751X07035598
19. X.H. Guo, B. Liu, M.H. Weng, Vacuum fluctuation effects on asymmetric nuclear matter. Phys. Rev. C **79**, 054316 (2009). doi:10.1103/PhysRevC.79.054316
20. C. Wu, Z. Ren, Strange hadronic stars in relativistic mean-field theory with the FSUGold parameter set. Phys. Rev. C **83**, 025805 (2011). doi:10.1103/PhysRevC.83.025805
21. C. Wu, W.L. Qian, Y.G. Ma et al., Neutron stars with kaon condensation in relativistic effective model. Int. J. Mod. Phys. E **22**, 1350026 (2013). doi:10.1142/S0218301313500262
22. H. Kurasawa, T. Suzuki, Effects of the Dirac sea on the Coulomb sum value for electron scattering. Nucl. Phys. A **490**, 571–584 (1988). doi:10.1016/0375-9474(88)90014-0
23. J. Antoniadis, P.C.C. Freire, N. Wex et al., A massive pulsar in compact relativistic binary. Science **340**, 1233232 (2013). doi:10.1126/science.1233232
24. P.B. Demorest, T. Pennucci, S.M. Ransom et al., A two-solar-mass neutron star measured using Shapiro delay. Nature **467**, 1081–1083 (2010). doi:10.1038/nature09466
25. T. Zhao, Y. Yan, X.L. Luo et al., Study of rotational quark stars and hybrid stars based on the latest equation of state and observation data. Phys. Rev. D **91**, 034018 (2015). doi:10.1103/PhysRevD.91.034018